International Journal of Engineering

Journal Homepage: www.ije.ir

An Investigation on Effects of Magnetic Parameter and Brownian Motion on Fluid Flow Between two Equal Plates: Application of Analytical Methods

P. Pasha[a], H. Nabi[a], M. M. Peiravi[b], M. Pourfallah[a], D. D. Ganji*[b]

[a] *Department of mechanical Engineering Mazandaran University of science and Technology, Babol, Iran*
[b] *Department of mechanical Engineering Babol Noshirvani University of Technology, Babol, Iran*

PAPER INFO

Paper history:
Received 26 july 2021
Received in revised form 28 August 2021
Accepted 29 August 2021

Keywords:
Adomian Decomposition Method
Brownian Motion
Hydrothermal Analysis
Thermo-phoretic

ABSTRACT

In the present paper, the heat transfer and fluid velocity between two horizontal plates is examined in existence of magnetic parameter. The parameters such as magnetic fluid flow, viscosity, Brownian motion, and thermo-phoretic have been investigated according to this analysis. The innovation of this paper is using two analytical methods to solve differential equations and compare the obtained results. In this paper, the effects of magnetic field on fluid flow for industrial use were investigated. The effects of magnetic field on fluid flow are surveyed by using Variation Iteration Method (VIM), Adomian Decomposition Method (ADM) and compare these methods with numerical Runge-Kutta method. According to results, increasing the values of magnetic parameter, the fluid velocity decreased and the fluid viscosity increased. Also, Brownian motion and thermo-phoretic parameters were directly related to the coefficient of friction. The Brownian motion of nanoparticles resulted in thermophoresis phenomenon and increasing both Brownian motion and thermophoresis causes an increase in temperature.

***doi**: 10.5829/ije.2021.34.10a.15*

NOMENCLATURE

H	distance the plates (m)	Nt	Thermo-phoretic parameter
C	Nano fluid concentration	Nb	Brownian motion
K	Dimensionless temperature	T_c	temperature of the cold wall (K)
x, y	coordinates (m)	ΔT	temperature difference
u,v	velocity components (m/s)	**Greek Symbols**	
θ	Dimensionless temperature	ρ	Density (kg/m^3)
ϑ	Kinematic viscosity (m^2/s)	$\boldsymbol{\mu}$	dynamic viscosity (kg/m. s)
C_p	Specific heat at constant pressure (J/kg.K)	$\boldsymbol{\beta}$	thermal expansion (1/K)
k	Thermal conductivity (W/m.K)	$\boldsymbol{\alpha}$	thermal diffusivity (m^2/s)
P^+	Modified fluid pressure	ν	Kinematic viscosity (m^2/s)
g_y	gravitational acceleration (m/s^2)	Ø	Dimensionless concentration
Pr	Prandtl number (υ/α)		

1. INTRODUCTION

Nanofluids are fluids containing Nano particle-sized fine particulate matter. Since these fluids have great heat transfer potential, special attention has been paid to this group of fluids as heat transfer environments.

Nanofluids have two parts. The first part is called the base fluid such as water and ethylene glycol, which is added to the mix. The second part of the Nanofluid is composed of Nanoparticles such as copper oxide and aluminum oxide. The major effects of Nanofluid and heat transfer through the Nanofluid can be attributed to the increase in energy efficiency, operating cost,

*Corresponding Author Institutional Email: ddg_davood@yahoo.com
(D. D. Ganji)

Please cite this article as: P. Pasha, H. Nabi, M. M. Peiravi, M. Pourfallah, D. D. Ganji, An Investigation on Effects of Magnetic Parameter and Brownian Motion on Fluid Flow Between two Equal Plates: Application of Analytical Methods, International Journal of Engineering, Transactions A: Basics Vol. 34, No. 10, (2021), 2341-2350

environmental clean up, or applications in the industry. The use of TiO_2-water nanofluids in the closed domain increases the Nusselt number by 23% and the friction factor by 42%. Grashof number is inversely related to increasing Nusselt number. mixed convection heat transfer from Al_2O_3-water nanofluid in W-shaped, copper tube cause the rate of heat transfer coefficient improved with Reynolds number for average wall temperatures of 50 and 60ºC. Magneto hydrodynamic nanofluid flow between two parallel analyzed and results showed concentration of nanofluid diminishes when Brownian movement increments whereas it increases with expands of thermophoretic parameter [1-20]. Gupta et al. [21] examined magneto convection in a nanofluid. Peiravi et al. [22] investigated the effect of variable Lorentz forces on nanofluid flow in movable parallel plates utilizing the analytical method. The results showed that increasing the Brownian motion parameter increased the temperature profile while increasing Brownian motion decreased the concentration profile. In the mentioned research, the influence of several factors, including skin friction coefficient, radiation parameter, and Weissenberg number was analyzed. An analytical investigation on mass and heat transfer of an MHD unsteady GO-water-squeezing nanofluid flow was carried out by Peiravi and Alinejad [23] between two infinite parallel moving plates. The novelty of this paper is the simultaneous simulation of two separate multi-phase nanofluids in two 3D enclosures under a heat flux boundary condition. Elsewhere, Pourmehran et al. [24] conducted an analytical study on squeezing unsteady nanofluid flow surrounded by parallel plates to which water (H_2O), as the base fluid mixed with several nanoparticles. Azimi and Mirzaei [25] performed an analytical study on the flow of Graphene oxide water nanofluid squeezed between parallel plates via RVIM. The results showed that the type of nanofluid is an important factor in the transfer of cooling and heating. As shown by Domairry Ganji et al. [26] the heat transfer rate increases in retention pools of nuclear waste. In another study by Hatami et al. [27] the differential quadrature method (DQM) was used to investigate the motion of a spherical particle in a fluid forced vortex. In this paper, the equations of particle motion in a forced vortex of fluid are calculated using the differential conversion method with Padé approximation. The velocity lines (angular and radial) and the path of a particle in a fluid vortex were examined in the present work. Rashidi et al. [28] investigated the flow point of the micropolar nanoscale. In this research, aluminum and copper oxides were used to prepare a mixture of water with basic liquids of Fe_3O_4 [29] nano cidal analysis in a porous environment under MHD. Modeling fluid and temperature fields were used the lattice Boltzmann approach based on the D2Q9 scheme. Jalilpour et al. [30] studied heat production at the MHD recession point of nanofluids to the porous tensile sheet. Hashemi Kachapi and Domairry Ganji [31] analyzed the nonlinear equations in fluids, progress in nonlinear science. In this work, they investigated various nonlinear equations by maple software. Aminoroayaie Yamini et al. [32] Mousavimehr et al. [33] Kostikov and Romanenkov [34] have examined the following issues. The first issue was the CFD model to investigate the hydraulic performance of the hole in the dam. In this research, the greatest speed for 100% opening of the door and Howell Bunger valve is almost 18 m/s within the area underneath the door, and the most extreme speed for 40% opening of the entryway is rise to 23.1 m/s. The second issue of article was the Performance Assessment of Shockwaves of Chute Spillways in Large Dams. In this article, the test arrangement of the shockwaves and their behavior along the chute and their lessening measures were displayed. The third subject of article was approximation of the multidimensional optimal control problem for the heat equation. The adomian decomposition method and variation iteration method are some of the most accurate tools for solving mathematical equations. These methods may be used to solve the ordinary differential equation and partial differential equation. In this paper, the nonlinear equations of velocity and temperature parameters were solved by using the adomian decomposition method (ADM) and Variation Iteration method. Also, it is tried to calculate the impacts of Brownian motion, viscosity factor, magnetic parameter, and thermophoretic factor on velocity and temperature. The innovations of this paper is the simulation of the results of Parameters the magnetic fluid flow, viscosity, Brownian motion, and thermo-phoretic using two numerical methods and compare these methods with the numerical method.

1. 1. Problem Definition Non-uniform flow is a flow that passes through two parallel plates and is affected by magnetic flux. Both the plate and the fluid stream rotate around y- axis. According to Figure 1, the plate is positioned at y=0 by two forces that are pulled to the opposite side of the plate. The direction of the magnetic flow is also along with the flow around the y-axis:

$$\frac{\partial u^+}{\partial x}+\frac{\partial v^+}{\partial y} \tag{1}$$

$$\rho_f\left(u^+\frac{\partial u^+}{\partial x}+V^+\frac{\partial u^+}{\partial y}\right)=-\frac{\partial P^+}{\partial x}+\mu\left(\frac{\partial^2 u^+}{\partial x^2}+\frac{\partial^2 u^+}{\partial y^2}\right)-\sigma B^2{}_0 u^+ \tag{2}$$

$$\rho_f\left(u^+\frac{\partial V^+}{\partial x}+V^+\frac{\partial V^+}{\partial y}\right)=-\frac{\partial P^+}{\partial y}+\mu\left(\frac{\partial^2 V^+}{\partial x^2}+\frac{\partial^2 V^+}{\partial y^2}\right) \tag{3}$$

$$\left(u^+\frac{\partial T^+}{\partial x}+V^+\frac{\partial T^+}{\partial y}\right)=\alpha\left(\frac{\partial^2 T^+}{\partial x^2}+\frac{\partial^2 T^+}{\partial y^2}\right)+\frac{(\rho C_p)_P}{(\rho C_P)_f}\times [D_B\left(\frac{\partial C^+}{\partial x}.\frac{\partial T^+}{\partial x}+\frac{\partial C^+}{\partial y}.\frac{\partial T^+}{\partial y}\right)+(\frac{D_T}{T_C^+})((\frac{\partial T^+}{\partial x})^2+\left(\frac{\partial T^+}{\partial y}\right)^2\Big] \tag{4}$$

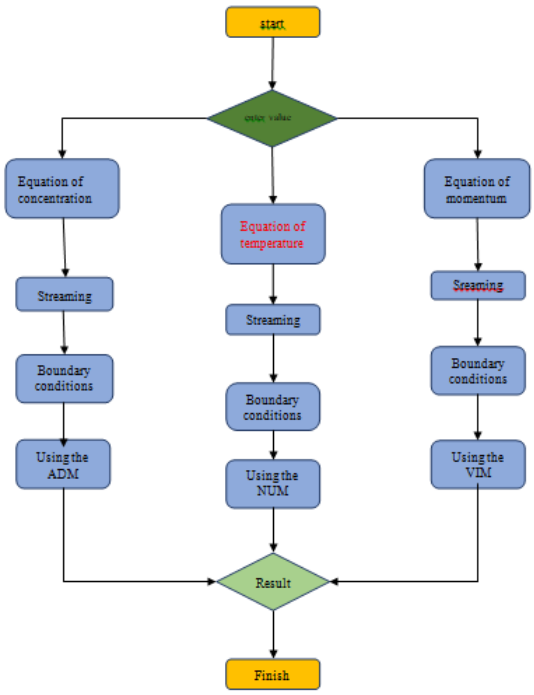

Figure 1. Flowchart of the problem

$$u^{+}\frac{\partial C^{+}}{\partial x}+V^{+}\frac{\partial C^{+}}{\partial y}=D_B\left(\frac{\partial^2 C^{+}}{\partial x^2}+\frac{\partial^2 C^{+}}{\partial y^2}\right)+\left(\frac{D_T}{T_0^{+}}\right)\left(\frac{\partial^2 T^{+}}{\partial x^2}+\frac{\partial^2 T^{+}}{\partial y^2}\right) \quad (5)$$

U^{+} And $V^{+}$are the velocities along the x-axis and y-axis, respectively. μ Denotes viscosity, $P^{+}$is modified fluid pressure, ρ_f is density,C^{+} is the specific heat of the nanofluid, K is the thermal conductivity, D_B is the diffusion coefficient of the diffusing species, and $T^{+}$is the temperature. The boundary conditions of these equations are as follows:

$$y=0 \leftrightarrow u^{+}=ax, T^{+}=T_h^{+}, V^{+}=0, C^{+}=C_h^{+} \quad (6)$$

$$y=h \leftrightarrow u^{+}=0, T^{+}=T_0^{+}, V^{+}=0, C^{+}=C_0^{+} \quad (7)$$

Non-dimensional variable in the above sentences is expressed as:

$$\eta=\frac{y}{h},\quad u^{+}=axf'(\eta),\quad V^{+}=-ahf(\eta),\quad \theta(\eta)=\frac{T^{+}-T_h^{+}}{T_0^{+}-T_h^{+}},\ \emptyset(\eta)=\frac{C^{+}-C_h^{+}}{C_0^{+}-C_h^{+}} \quad (8)$$

Now, we can write a genuine equation:

$$f^{(4)}-R(f'f''-ff'')-Mf''=0 \quad (9)$$

$$\theta''+PrRf\theta'+Nb\emptyset'\theta'+Nt\theta'^{2}=0 \quad (10)$$

$$\emptyset''+R.Scf\emptyset'+\frac{Nt}{Nb}\theta''=0 \quad (11)$$

The new boundary conditions are:

$$\eta=0\rightarrow f=0, f'=1, (\theta=1, \emptyset=1) \quad (12)$$

$$\eta=1\rightarrow f=1, (f'=0, \theta=0, \emptyset=0) \quad (13)$$

Dimensionless quantities: Nt is the thermo phoretic gauge, M is the magnetic gauge, Pr is a Prandtl number, R is the viscosity coefficient, Nb is the Brownian motion gauge and Sc is the Schmidt number.

$$R=\frac{ah^2}{\vartheta}, M=\frac{\sigma B_0 B_0 h^2}{\rho\vartheta}, Pr=\frac{\mu}{\rho_f\alpha}, Sc=\frac{\mu}{\rho_f D}, Nt=(\rho C)_P D_T(T_h^{+})/(\rho C)_f\alpha T_c^{+}, Nb=(\rho C)_P D_B(C_h)/(\rho C)_f\alpha \quad (14)$$

Nusselt number is defined as:

$$Nu=-\theta' \quad (15)$$

3. SIMULATION METHODOLOGY

3. 1. A. Adomian Decomposition Method (ADM)

A general nonlinear equation is considered in the form of [31]:

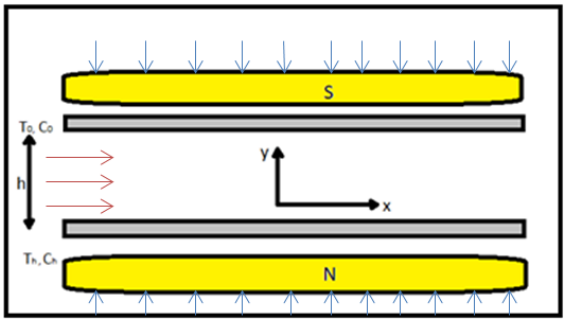

Figure 2. Schematic of magnetic effects between horizontal plates on Brownian motion

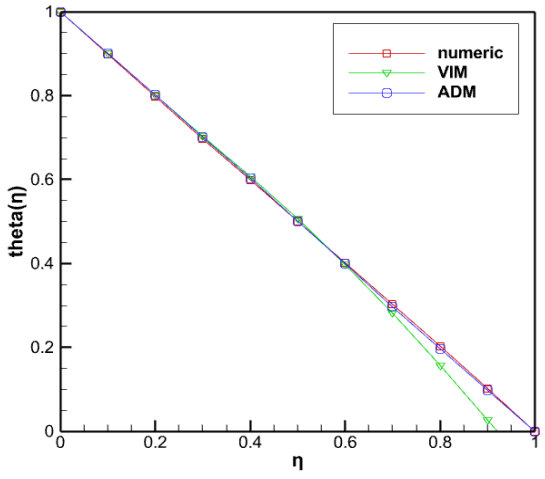

(a) Temperature profile

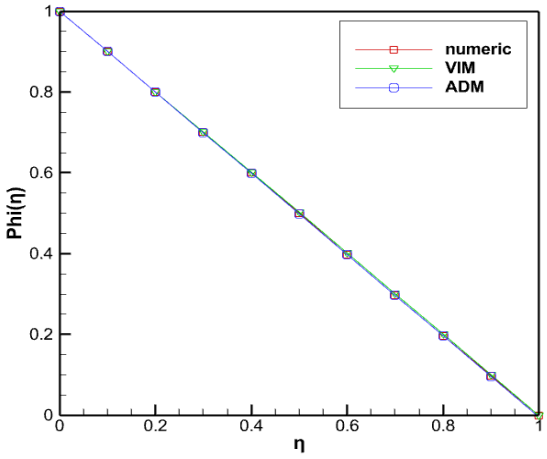

(b) Concentration profile

Figure 3. Comparison of a) the temperature and b) the concentration profile between ADM and VIM and Runge-Kutta methods at M=1, R=1, Sc=0.1, Nt=0.1, Nb=0.1, Pr=2.

$$L(u)+Ru+Nu=g(r) \quad (16)$$

Applying the inverse operator L^{-1} to both sides of (16) and using the given conditions [31]:

$$U=f(x)-L^{-1}(Ru)-L^{-1}(Nu) \quad (17)$$

For nonlinear differential equations, the nonlinear operator Nu=F(u) is observed in the Adomian decomposition method [5]:

$$F(u)=\sum_{m=0}^{\infty} A_m \quad (18)$$

The Adomian method defines the solution U(x) by the series [31]:

$$u=\sum_{m=0}^{\infty} u_m \quad (19)$$

$$F(u)=F(u_0)+F'(u_0)(u-u_0)+F''(u_0)\frac{(u-u_0)}{2!}+F'''(u_0)\frac{(u-u_0)}{3!}+\cdots \quad (20)$$

By equating terms, the first few Adomian polynomials $A_0, A_1, A_2,\ldots$[5]:

$$A_0=F(u_0) \qquad A_1=u_1F'(u_0) \qquad A_2=u_2F'(u_0)+\frac{1}{2!}u_1u_1F''(u_0) \quad (21)$$

3. 2. Application of ADM Based on ADM, the linear parts of the equation were divided and set it to 0. The differential equation with boundary conditions were solved.

$$\frac{d^4}{d\eta^4}f_0(\eta)=0 \quad (22)$$

$$\frac{d^2}{d\eta^2}\theta_0(\eta)=0 \quad (23)$$

$$\frac{d^2}{d\eta^2}\emptyset_0(\eta)=0 \quad (24)$$

$$f_0(\eta)=\eta^2-2\eta^2+\eta \leftrightarrow \theta_0(\eta)=\eta+1 \leftrightarrow \emptyset_0(\eta)=\eta+1 \quad (25)$$

Then, the non-linear differential equations are separated for Equation (9):

$$A_0=-R(3\eta^2-4\eta+1)(6\eta-4) \quad (26)$$

$$B_0=R(\eta^2-2\eta^2+\eta)(6\eta-4) \quad (27)$$

$$C_0=-M(6\eta-4) \quad (28)$$

$$A_1=(-R(6\eta-4)^2-6R(3\eta^2-4\eta+1))f_1(\eta) \quad (29)$$

$$B_1=(R(3\eta^2-4\eta+1)(6\eta-4)+6R(\eta^3-2\eta^2+\eta))f_1(\eta) \quad (30)$$

$$C_1=-6Mf_1(\eta) \quad (31)$$

For Equation (10):

$$D_0=-Pr\,R\,(\eta^3-2\eta^2+\eta) \quad (32)$$

$$D_1=-Pr\,R(3\eta^2-4\eta+1)\theta_1(\eta) \quad (33)$$

For Equation (11):

$$E_0=-R\,Sc\,(\eta^3-2\eta^2+\eta) \quad (34)$$

$$E_1=-R\,Sc(3\eta^2-4\eta+1)\emptyset_1(\eta) \quad (35)$$

According to the ADM method, the following statements of the parameters of the equations were written:

$$F_1(\eta)=R\left(\frac{3}{140}\eta^7-\frac{1}{10}\eta^6+\frac{11}{60}\eta^5-\frac{1}{6}\eta^4\right)-R\left(\frac{1}{280}\eta^8-\frac{2}{105}\eta^7+\frac{7}{180}\eta^6-\frac{1}{30}\eta^5\right)+M\left(\frac{1}{20}\eta^5-\frac{1}{6}\eta^4\right) \quad (36)$$

$$\theta_1(\eta)=-Pr\,R\left(\frac{1}{20}\eta^5-\frac{1}{6}\eta^4+\frac{1}{6}\eta^3\right)+\frac{1}{2}Nb\eta^2+\frac{1}{2}Nt\eta^2 \quad (37)$$

$$\emptyset_1(\eta)=-R\,Sc\left(\frac{1}{20}\eta^5-\frac{1}{6}\eta^4+\frac{1}{6}\eta^3\right) \quad (38)$$

Next, adding two sentences from each equation at M=1, Pr=2, R=1, Sc=0.1, Nt=0.1 and Nb=0.1 give:

$$F(\eta)=f_0(\eta)+f_1(\eta)\rightarrow f(\eta)=\eta^3-2\eta^2+\eta+\frac{17}{420}\eta^7-\frac{5}{36}\eta^6+\frac{4}{15}\eta^5-\frac{1}{3}\eta^4-\frac{1}{280}\eta^8 \quad (39)$$

$$\theta(\eta)=\theta_0(\eta)+\theta_1(\eta)\rightarrow\theta(\eta)=-\eta+1-\frac{1}{10}\eta^5+\frac{1}{3}\eta^4-\frac{1}{3}\eta^3+0.10\eta^2 \quad (40)$$

$$\emptyset(\eta)=\emptyset_0(\eta)+\emptyset_1(\eta)\rightarrow\emptyset(\eta)=-\eta+1-0.005\eta^5+0.016\eta^4-0.016\eta^3+0.000021\eta^9-0.000125\eta^8+0.00029\eta^7-0.00028\eta^6$$

3. 3. Variation Iteration Method (VIM) Where Ω is the frequency angle oscillator. The general formula for obtaining other sentences of u is defined by a coefficient λ as follows [31]:

$$u' + \Omega^2 = F(u)$$
$$F(u) = \Omega^2 u - \mathrm{f}(u) \quad (41)$$

Given the boundary equations:

$$u' = 0,$$
$$u(0) = \mathrm{A} \quad (42)$$

And the first functions:

$$u_0(\mathrm{t}) = \mathrm{A}\cos\Omega \quad (43)$$

$$\int_0^{\mathrm{T}} \cos\Omega \mathrm{t}[\Omega^2 \mathrm{u}_0 - \mathrm{f}(\mathrm{u}_0)]\mathrm{dt} = 0 \quad (44)$$

The λ coefficient is obtained by dividing the Laplace from the linear part of the equation. By different n definitions, the number of sentences is considered to obtain a better answer:

$$u_{n+1}(t) = u_n(t) + \int_0^{\mathrm{t}} \lambda \left\{ \frac{\mathrm{d}^2 \mathrm{u}_n}{\mathrm{d}\eta^2} + \Omega^2 \mathrm{u}_{\mathrm{n}}(\eta) - \mathrm{F}_n \right\} \mathrm{d}\eta \quad (45)$$

where λ is the Lagrange coefficient and F_n is considered various restricted:

$$\frac{d^2\lambda}{d\eta^2} + \Omega^2 \lambda(\eta) = 0 \quad (46)$$

$$\lambda(t) = 0, \quad (47)$$

$$1 - \frac{d\lambda}{dt} = 0 \quad (48)$$

The coefficient λ is calculated from the following formula:

$$\lambda = \frac{1}{\Omega} sin\Omega(\tau - t) \quad (49)$$

Then the formula is rewritten:

$$u_{n+1}(t) = u_n(t) + \int_0^t \frac{1}{\Omega} sin\Omega(\tau - t) \left\{ \frac{d^2 u_n}{d\eta^2} + F_n \right\} d\tau \quad (50)$$

3. 4. Application of VIM Based on the VIM method, the linear parts of the coupling equations are written as follows:

$$\frac{d^4}{d\eta^4} \mathrm{f}_0(\eta) = 0 \quad (51)$$

$$\frac{d^2}{d\eta^2} \theta_0(\eta) = 0 \quad (52)$$

$$\frac{d^2}{d\eta^2} \emptyset_0(\eta) = 0 \quad (53)$$

Then, the boundary conditions for the linear parts are expressed in the following:

$$F_0(0) = 0, \ f_0'(0) = 1, \ \theta_0(0) = 1, \ \emptyset_0(0) = 1 \quad (54)$$

$$f_0(1) = 0, \ \theta_0(1) = 0, \ \emptyset_0(1) = 0, \ f_0'(1) = 0 \quad (55)$$

The first sentences are given in terms of f and θ and $\emptyset$:

$$f_0(\eta) = \eta^3 - 2\eta^2 + \eta \ , \theta_0(\eta) = \eta + 1, \emptyset_0(\eta) = \eta + 1 \quad (56)$$

Then, by computing the linear parts of the equations, $\lambda_1, \lambda_2,$ and λ_3 are calculated as follows:

$$\lambda_1 = \frac{1}{6}(\tau - \eta)^3 \quad (57)$$

$$\lambda_2 = \tau - \eta \quad (58)$$

$$\lambda_3 = \tau - \eta \quad (59)$$

$$f_1(\eta) = \eta^3 - 2\eta^2 + \eta + \frac{1}{4}\left(-\frac{1}{6}R\left((3\eta^2 - 4\eta + 1)(6\eta - 4) - (\eta^3 - 2\eta^2 + \eta)(6\eta - 4)\right) - \frac{1}{6}M(6\eta - 4)\right)\eta^4 - \frac{1}{12}\eta^4\left(-R\left((3\eta^2 - 4\eta + 1)(6\eta - 4) - (\eta^3 - 2\eta^2 + \eta)(6\eta - 4)\right) - M(6\eta - 4)\right) \quad (60)$$

$$\theta_1(\eta) = -\eta + 1 - \frac{1}{2}\left(-Pr\ R(\eta^3 - 2\eta^2 + \eta) + Nb + Nt\right)\eta^2 \quad (61)$$

$$\emptyset_1(\eta) = -\eta + 1 + \frac{1}{2} R\ Sc\ (\eta^3 - 2\eta^2 + \eta)\eta^2 \quad (62)$$

Finally, by summing up the sentences at M=1, Pr=10, R=1, Sc=0.1, Nt=0.1, and Nb=0.1:

$$f(\eta) = f_1(\eta) \to f(\eta) = \eta^3 - 2\eta^2 + \eta + \frac{17}{12}\eta^7 - \frac{25}{12}\eta^6 + \frac{4}{3}\eta^5 - \frac{1}{3}\eta^4 - \frac{1}{4}\eta^8 \quad (63)$$

$$\theta(\eta) = (\eta + 0.8104) \times (\eta - 0.9203) \times (\eta - 1.4650) \times (\eta^2 - 0.4253) \times (\eta + 0.9153) \quad (64)$$

$$\emptyset(\eta) = \emptyset_1(\eta) \to \emptyset(\eta) = 0.5(\eta + 1.9029) \times (\eta - 1) \times (\eta - 2.4168) \times (\eta^2 - 0.4860) \times (\eta + 4.3490) \quad (65)$$

3. 5. Runge-Kutta Methods Runge-Kutta methods are a family of iterative methods used to match solutions to ordinary differential equations (OED). These methods use discretization in computing solutions in small steps. The next step Approximation is derived from the previous step by adding s terms. A problem of initial value should be specified as follows:

$$k_1 = h\, f(x_n, y_n) \quad (66)$$

$$k_2 = h\, f(x_n + \frac{1}{2}h\, , y_n + \frac{1}{2}k_1) \quad (67)$$

$$k_3 = h\, f(x_n + \frac{1}{2}h\, , y_n + \frac{1}{2}k_2) \quad (68)$$

$$k_4 = h\, f(x_n + h\,, y_n + k_3) \tag{69}$$

$$y_{n+1} = y_n + \frac{1}{6}k_1 + \frac{1}{3}k_2 + \frac{1}{3}k_3 + \frac{1}{6}k_4 + O(h^5) \tag{70}$$

k_1 is the slope at the start of the space using y. k_2 is the gradient in the middle of the range using y and k_1. k_3 is again the mid-course gradient but using y and k_2. k_4 is the slope at the end of the range utilizing y and k_3.

3. 6. Validation for Analytical Methods Figure 2 indicates the convergence graph of temperature and concentration profile in the range 0 to 1. Here, by applying two analytical solution methods and comparing the results with the numerical solution, the concentration and temperature parameters are evaluated. As shown in Figure 2, the ADM and numeric solutions converged on a line, but the VIM method initially had some numerical error, but began to converge on a line and converged with them. The third form converged without any computational error of all methods.

In this section for validation in accordance to Table 1, the present study compared to Derakhshan et al. [5]. The amount of computational error in our work is very low compared to others.

4. RESULTS AND DISCUSSION

In this research, the Nanofluids flow between two parallel plates is investigated using the ADM and VIM approach. Several diagrams according to Brownian motion, viscosity, thermophoresis factor, and magnetic influence relative to η were used to investigate fluid flow and heat transfer. A comparison was also made between the obtained results and the numerical method findings. The effect of the magnetic force having viscous impacts on Nanofluidic flow is presented in Figs. 4, 5, and 6. The comparative of results of ADM and NUM and VIM methods for investigating the effect of MHD and Viscosity on the temperature and velocity profiles. As can be seen in Figure 3, increasing the distance from the plate to the top, leads to a reduction in heat transfer and concentration. Based on Figure 4, by increasing the magnetic effects viscosity and velocity reduced and temperature is increased. Figure 5 shows the velocity changes of the fluid relative to viscosity changes. According to this graph, when the viscosity parameter increased, the fluid velocity decreased. Figure 6 shows the temperature changes of the fluid relative to viscosity changes. Based on this picture, the temperature profile reduces as a result of increasing the viscosity factor. Figure 7 shows the temperature changes of the fluid relative to thermophoretic parameter changes. The effects of the thermo-phoretic parameter and Brownian motion on the temperature are also presented in Figs. 7 and 8. The increase in thermo-phoretic parameters and Brownian motion has been found to increase temperature. The Brownian motion of nanoparticles results in the thermophoresis phenomenon, and increasing both Brownian motion and thermophoresis causes an increase in temperature. Figure 8 shows an increased concentration profile by increasing the viscosity factor. The heat transfer from fluid flow to surface increased by increasing concentration coefficient. Thermophoresis has caused by the Brownian motion of nanoparticles in fluids with a continuous temperature differential that is maintained externally. Because of the temperature disparity in the suspensions flow zone, tiny particles scatter faster in the hotter domain and slower in the colder domain. The cumulative impact of nanoparticle dispersion is migration from a hotter to a colder location of the fluid domain. According to Figure 9, by increasing the amount of viscosity the concentration parameter increased. This result is the same for both methods.

Figure 10 demonstrates the influences of the Schmidt number on the concentration profile (∅), and according

TABLE 1. Numerical comparison of non-dimensional temperature profile between present work with Derakhshan et al work [5]

η	$\theta_{Present}$	$\theta_{Derakhshan}$
0	1	1
0.1	0.9006990000	0.899450520215274
0.2	0.8018346666	0.798446158109890
0.5	0.5010416666	0.499408530656464
0.8	0.1970986666	0.203135052008296
0.9	0.09765100000e-1	0.102480354104553
1	0	0

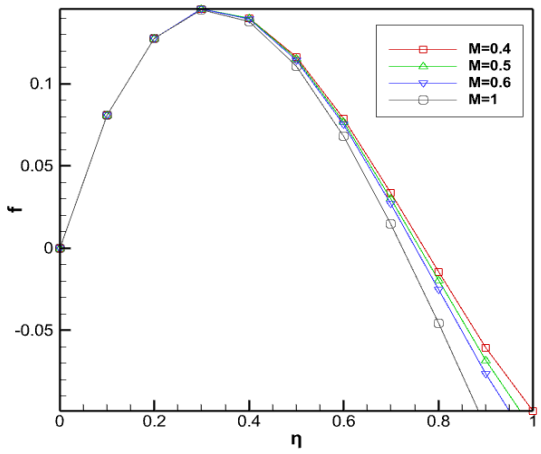

Figure 4. Effect of MHD on profile velocity by ADM at Pr=2, Sc=0.1, Nt=0.1, Nb=0.1

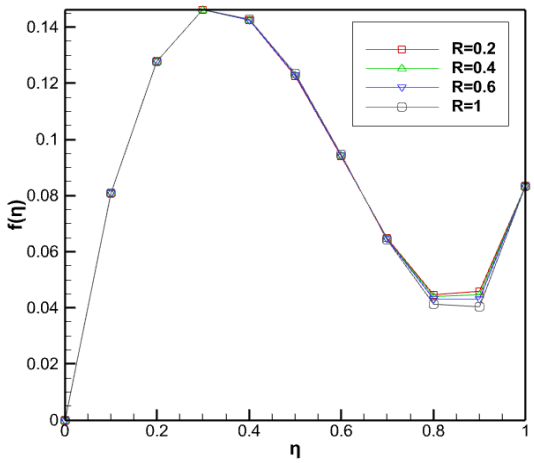

Figure 5. Effect of Viscosity on profile velocity by VIM at Pr=2, Sc=0.1, Nt=0.1, Nb=0.1

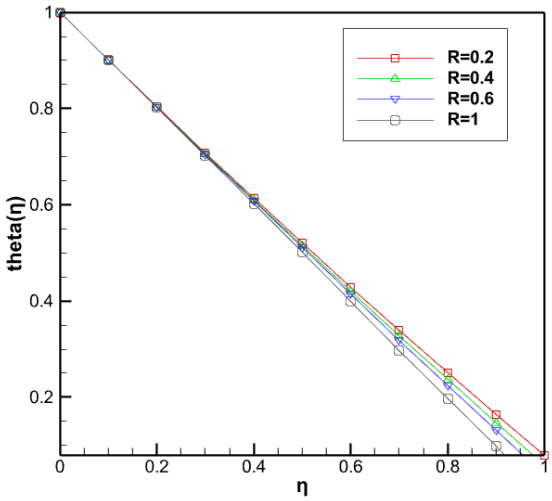

Figure 6. Effect of viscosity on profile temperature by ADM at Pr=2, M=1, Sc=0.1, Nt=0.1, Nb=0.1

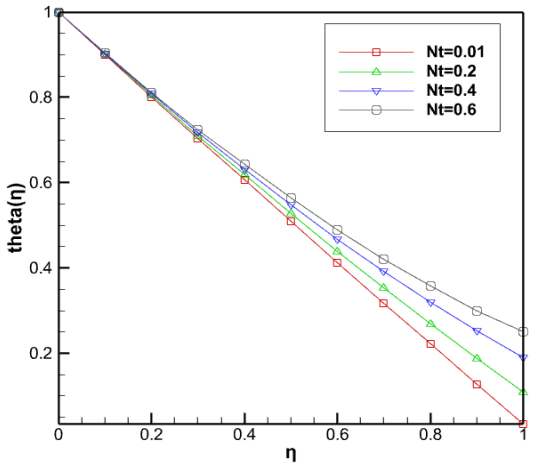

Figure 7. Effect of thermo-phoretic parameter on temperature by ADM method at Pr=2, M=1, Sc=0.1,Nb=0.1

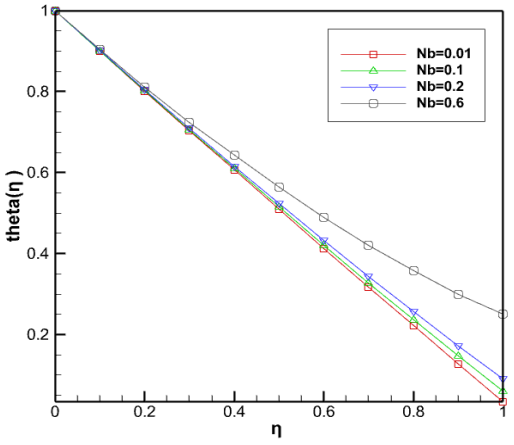

Figure 8. Influence of Brownian parameter on Temperature by ADM method at Pr=2, M=1, Sc=0.1, Nb=0.1

to the figure, by increasing the Schmidt number of fluid flow, the concentration parameter decreased.

Tables 2 and 3 summarized a numerical comparison of non-dimensional temperature and concentration

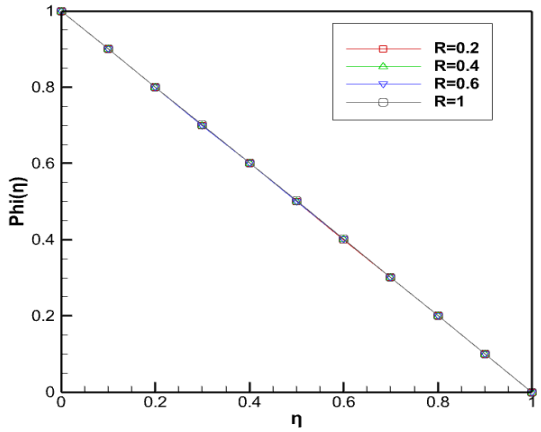

(a) ADM

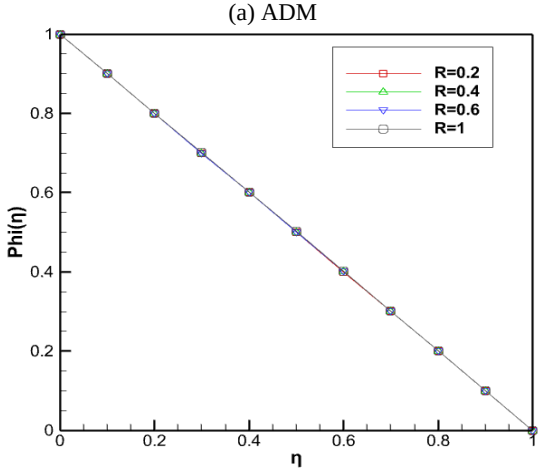

(b) VIM

Figure 9. Effect of viscosity on profile concentration by a) ADM and b) VIM at Pr=2, M=1, Sc=0.1, NT=0.1, Nb=0.1

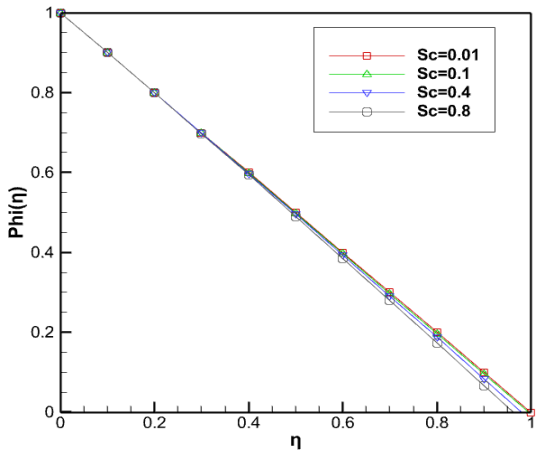

(a) ADM

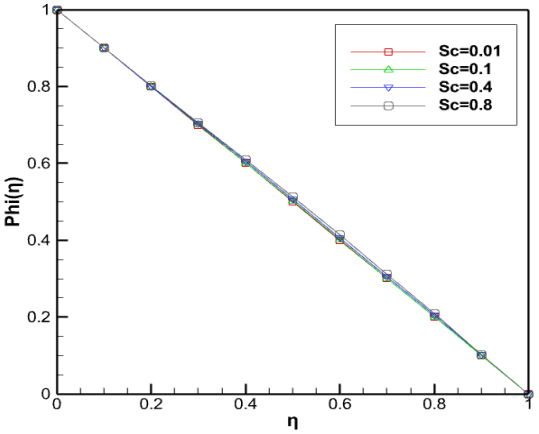

(b) VIM

Figure 10. Influence of Schmidt number on concentration by a) ADM and b) VIM method at Pr=2, M=1, Nt=0.1, Nb=0.1

TABLE 2. Numerical comparison of non-dimensional temperature between ADM, VIM and Runge-Kutta method

η	θ_{ADM}	θ_{VIM}	$\theta_{NUMERIC}$
0	1	1	1
0.1	0.9006990000	0.899450520215	0.899450
0.2	0.8018346666	0.798446158109	0.798446
0.5	0.5010416666	0.499408530656	0.499408
0.8	0.1970986666	0.203135052008	0.203135
0.9	0.0976510000	0.102480354104	0.102480
1	0	0	0

profile between ADM, VIM, and Runge-Kutta methods. In this section, all calculations are calculated with the least error.

According to Table 4, the specifications of the system used to solve the equations are as follows.

TABLE 3. Numerical comparison of non-dimensional Concentration profile between ADM, VIM and Runge-Kutta method

η	$\emptyset_{ADM}$	$\emptyset_{VIM}$	$\emptyset_{NUMERIC}$
0	1	1	1
0.1	0.8906990000	0.909450520215	0.909450
0.2	0.7918346666	0.808446158109	0.808446
0.5	0.4910416666	0.509408530656	0.499408
0.8	0.1970986666	0.203135052008	0.193135
0.9	0.0956510000	0.102480354104	0.972480
1	0	0	0

TABLE 4. comparison of CPU time between ADM and VIM

Numerical method	ADM	VIM
CPU time	2.77(s)	7.50(s)

Computer RAM =8, CPU=core i7. According to Table 3, the ADM method was obtained faster than VIM method.

5. CONCLUSION

In this paper, the heat transfer and fluid velocity between two horizontal plates is examined in existence of magnetic parameter. The parameters such as magnetic fluid flow, viscosity, Brownian motion, and thermo-phoretic have been investigated according to this analysis. The innovation of this paper is the using of two analytical methods for calculate differential equations and comparison these results with together. The results showed Temperature rise is accompanied by increases in the magnetic factor and reduction in concentration profile. Also, when Brownian motion increased, the viscosity parameter decreases. Brownian motion and thermo-phoretic parameters were directly related to the coefficient of friction.

- The velocity of the fluid between 2 plates with increasing the influence of the magnetic force from M=0.4 to M=1 is generally reduced.
- Influence of thermo-phoretic parameter on Temperature by ADM and VIM methods show that by increasing Nt=0.01 to Nt=0.6, The temperature increases from θ=0 to θ=0.28.
- By increasing the Schmidt number of fluid flow, the concentration parameter decreased.
- Thermophoresis is caused by the Brownian motion of nanoparticles in fluids with a continuous temperature differential that is maintained externally.

6. REFERENCES

1. Adibi, T., Razavi, S.E. and Adibi, O., "A characteristic-based numerical simulation of water-titanium dioxide nano-fluid in closed domains", ***International Journal of Engineering***, Vol. 33, No. 1, (2020), 158-163, doi: 10.5829/IJE.2020.33.01A.18.
2. Sadripour, S., "Investigation of flow characteristics and heat transfer enhancement in a nanofluid flow in a corrugated duct", ***Journal of Applied Mechanics and Technical Physics***, Vol. 59, No. 6, (2018), 1049-1057, doi: 10.1134/S002189441806010X.
3. Loganathan, P., Chand, P.N. and Ganesan, P., "Transient natural convective flow of a nanofluid past a vertical plate in the presence of heat generation", ***Journal of Applied Mechanics and Technical Physics***, Vol. 56, No. 3, (2015), 433-442, doi: 10. 1134/ s002189441503013x.
4. Razmara, N., "Microstructure of the poiseuille flow in a model nanofluid by molecular dynamics simulation", ***Journal of Applied Mechanics and Technical Physics***, Vol. 56, No. 5, (2015), 894-900, doi: 10.1134/S002189441505017X.
5. Derakhshan, R., Shojaei, A., Hosseinzadeh, K., Nimafar, M. and Ganji, D., "Hydrothermal analysis of magneto hydrodynamic nanofluid flow between two parallel by agm", ***Case Studies in Thermal Engineering***, Vol. 14, (2019), 100439, doi: 10.1016/j.csite.2019.100439.
6. Humphries, U., Govindaraju, M., Kaewmesri, P., Hammachukiattikul, P., Unyong, B., Rajchakit, G., Vadivel, R. and Gunasekaran, N., "Analytical approach of fe3o4-ethylene glycol radiative magnetohydrodynamic nanofluid on entropy generation in a shrinking wall with porous medium", ***International Journal of Engineering***, Vol. 34, No. 2, (2021), 517-527, doi. https://dx.doi.org/10.5829/ije.2021.34.02b.25
7. Mobadersani, F. and Bahjat, S., "Magnetohydrodynamic (mhd) flow in a channel including a rotating cylinder", ***International Journal of Engineering***, Vol. 34, No. 1, (2021), 224-233, doi. https://dx.doi:org/10.5829/ije.2021.34.01a.25
8. Akbarzadeh, P. and Fardi, A., "Natural convection heat transfer in 2d and 3d trapezoidal enclosures filled with nanofluid", ***Journal of Applied Mechanics and Technical Physics***, Vol. 59, No. 2, (2018), 292-302, doi: 10.1134/S0021894418020128.
9. Shahriari, A., Jahantigh, N. and Rakani, F., "Assessment of particle-size and temperature effect of nanofluid on heat transfer adopting lattice boltzmann model", ***International Journal of Engineering***, Vol. 31, No. 10, (2018), 1749-1759, doi: 10.5829/ije.2018.31.10a.18.
10. Alagappan, N. and Karunakaran, N., "Performance investigation of 405 stainless steel thermosyphon using cerium (iv) oxide nano fluid", ***International Journal of Engineering***, Vol. 30, No. 4, (2017), 575-581, doi: 10.5829/idosi.ije.2017.30.04a.16.
11. Akbari, M., Yavari, M., Nemati, N., Babaee Darband, J., Molavi, H. and Asefi, M., "An investigation on stability, electrical and thermal characteristics of transformer insulting oil nanofluids", ***International Journal of Engineering***, Vol. 29, No. 10, (2016), 1332-1340, doi: 10.5829/idosi.ije.2016.29.10a.02.
12. AJAY, K., "Performance evaluation of nanofluid (al2o3/h2o-c2h6o2) based parabolic solar collector using both experimental and cfd techniques", ***International Journal of Engineering***, Vol. 29, No. 4, (2016), 572-580, doi: 10.5829/idosi.ije.2016.29.04a.17.
13. Kheiri, M. and Davarnejad, R., "Numerical comparison of turbulent heat transfer and flow characteristics of sio2/water nanofluid within helically corrugated tubes and plain tube", ***International Journal of Engineering***, Vol. 28, No. 10, (2015), 1408-1414, doi: 10.5829/idosi.ije.2015.28.10a.02.
14. Khan, D., Hakim, M.A. and Alam, M., "Analysis of magneto-hydrodynamics jeffery-hamel flow with nanoparticles by hermite-padé approximation", ***International Journal of Engineering***, Vol. 28, No. 4, (2015), 599-607, doi: 10.5829/idosi.ije.2015.28.04a.15.
15. Goshtasbi Rad, E., "Experimental investigation of mixed convection heat transfer in vertical tubes by nanofluid: Effects of reynolds number and fluid temperature", ***International Journal of Engineering***, Vol. 27, No. 8, (2014), 1251-1258, doi: 10.5829/idosi.ije.2014.27.08b.11.
16. Mohammadi Ardehali, R., "Modeling of tio2-water nanofluid effect on heat transfer and pressure drop", ***International Journal of Engineering***, Vol. 27, No. 2, (2014), 195-202, doi: 10.5829/idosi.ije.2014.27.02b.04.
17. Rostami, M., Hassani Joshaghani, A., Mazaheri, H. and Shokri, A., "Photo-degradation of p-nitro toluene using modified bentonite based nano-tio2 photocatalyst in aqueous solution", ***International Journal of Engineering***, Vol. 34, No. 4, (2021), 756-762, doi. https://dx.doi.org/10.5829/ije.2021.34.04a.01
18. Siavashy, O.S., Nabian, N. and Rabiee, S., "Titanium dioxide nanotubes incorporated bioactive glass nanocomposites: Synthesis, characterization, bioactivity evaluation and drug loading", ***International Journal of Engineering***, Vol. 34, No. 1, (2021), 1-9, doi. https://dx.doi.org/10.5829/ije.2021.34.01a.01
19. Taheri, A.A. and Taghilou, M., "Towards a uncertainty analysis in thermal protection using phase-change micro/nano particles during hyperthermia", ***International Journal of Engineering***, Vol. 34, No. 1, (2021), 263-271, doi: 10.5829/ije.2021.34.01a.29.
20. Peiravi, M.M., Alinejad, J., Ganji, D. and Maddah, S., "Numerical study of fins arrangement and nanofluids effects on three-dimensional natural convection in the cubical enclosure", ***Challenges in Nano and Micro Scale Science and Technology***, Vol. 7, No. 2, (2019), 97-112, doi: 10.22111/tpnms.2019.27933.1164.
21. Gupta, U., Ahuja, J. and Wanchoo, R., "Magneto convection in a nanofluid layer", ***International Journal of Heat and Mass Transfer***, Vol. 64, (2013), 1163-1171, doi: 10.1016/j.ijheatmasstransfer.2013.05.035.
22. Peiravi, M.M., Alinejad, J., Ganji, D.D. and Maddah, S., "3d optimization of baffle arrangement in a multi-phase nanofluid natural convection based on numerical simulation", ***International Journal of Numerical Methods for Heat & Fluid Flow***, (2019), doi: 10.1108/HFF-01-2019-001.
23. Peiravi, M.M. and Alinejad, J., "Nano particles distribution characteristics in multi-phase heat transfer between 3d cubical enclosures mounted obstacles", ***Alexandria Engineering Journal***, Vol. 60, No. 6, (2021), 5025-5038, doi: 10.1016/j.aej.2021.04.013.
24. Pourmehran, O., Rahimi-Gorji, M., Gorji-Bandpy, M. and Ganji, D., *Retracted: Analytical investigation of squeezing unsteady nanofluid flow between parallel plates by lsm and cm*. 2015, Elsevier.
25. Azimi, A. and Mirzaei, M., "Analytical investigation of squeezing flow of graphene oxide water nanofluid between parallel plates using rvim", ***Journal of Computational and Theoretical Nanoscience***, Vol. 12, No. 2, (2015), 175-179, doi: 10.1166/jctn.2015.3711.
26. Domari, G.D., Peiravi, M. and Abbasi, M., "Evaluation of the heat transfer rate increases in retention pools nuclear waste", ***International Journal of Nano Dimension***, Vol. 6, No. 4, (2015), 385-398.
27. Hatami, M. and Ganji, D., "Motion of a spherical particle in a fluid forced vortex by dqm and dtm", ***Particuology***, Vol. 16, (2014), 206-212, doi: 10.1016/j.partic.2014.01.001.
28. Rashidi, M.M., Reza, M. and Gupta, S., "Mhd stagnation point flow of micropolar nanofluid between parallel porous plates with uniform blowing", ***Powder Technology***, Vol. 301, (2016), 876-885, doi: 10.1016/j.powtec.2016.07.019.

29. Peiravi, M.M. and Alinejad, J., "Hybrid conduction, convection and radiation heat transfer simulation in a channel with rectangular cylinder", ***Journal of Thermal Analysis and Calorimetry***, Vol. 140, No. 6, (2020), 2733-2747, doi: 10.1007/s10973-019-09010-0.

30. Jalilpour, B., Jafarmadar, S., Ganji, D., Shotorban, A. and Taghavifar, H., "Heat generation/absorption on mhd stagnation flow of nanofluid towards a porous stretching sheet with prescribed surface heat flux", ***Journal of Molecular Liquids***, Vol. 195, (2014), 194-204, doi: 10.1016/j.molliq.2014.02.021.

31. Ganji, D. and HashemiKachapi, S., "Analysis of nonlinear equations in fluids, progress in nonlinear science", ***Sian Academic***, , (2011), 1-294.

32. Aminoroayaie Yamini, O., Mousavi, S.H., Kavianpour, M. and Safari Ghaleh, R., "Hydrodynamic performance and cavitation analysis in bottom outlets of dam using cfd modelling", ***Advances in Civil Engineering***, Vol. 2021, (2021), doi: 10.1155/2021/5529792.

33. Mousavimehr, S., Yamini, O.A. and Kavianpour, M., "Performance assessment of shockwaves of chute spillways in large dams", ***Shock and Vibration***, Vol. 2021, (2021), doi: 10.1155/2021/6634086.

34. Kostikov, Y.A. and Romanenkov, A.M., "Approximation of the multidimensional optimal control problem for the heat equation (applicable to computational fluid dynamics (CFD))", ***Civil Engineering Journal***, Vol. 6, No. 4, (2020), 743-768, doi: 10.28991/cej-2020-03091506.

Persian Abstract

چکیده

در مقاله حاضر ، انتقال حرارت و سرعت سیال بین دو صفحه افقی با وجود پارامتر مغناطیسی بررسی شده است. پارامترهایی مانند جریان سیال مغناطیسی ، ویسکوزیته ، حرکت براونی و ترموفورتیک با توجه به این مورد بررسی شده است. نوآوری این مقاله استفاده از دو روش تحلیلی برای محاسبه معادلات دیفرانسیل و مقایسه این نتایج با هم میباشد.در این مقاله ، اثرات میدان مغناطیسی روی جریان سیال برای مصارف صنعتی مورد بررسی قرار گرفته است. اثرات میدان مغناطیسی جریان سیال با استفاده از روش تکرار تغییرات (VIM) و Adomian مورد بررسی قرار می گیرد و نتایج ان با روش نیومریک مقایسه میشود. مطابق با نتایج حاصله با افزایش اثرات مغناطیس ، سرعت جریان سیال کاهش می یابد و ویسکوزیته بیشتر میشود. همچنین ضریب نیروی براون با ضریب ترموفورتیک رابطه مستقیمی با ضریب اصطکاک دارند. نیروی براون نانوذرات نتایج ضریب ترموفورتیک هستند بطوریکه با افزایش نیروی براون و ترموفورتیک دما افزایش می یابد.